Defense Technical Information Center
Compilation Part Notice

ADP012854

TITLE: Electronic Properties and Many-Body Effects in Quantum Dots

DISTRIBUTION: Approved for public release, distribution unlimited
Availability: Hard copy only.

This paper is part of the following report:

TITLE: Nanostructures: Physics and Technology. 7th International
Symposium. St. Petersburg, Russia, June 14-18, 1999 Proceedings

To order the complete compilation report, use: ADA407055

The component part is provided here to allow users access to individually authored sections
of proceedings, annals, symposia, etc. However, the component should be considered within
the context of the overall compilation report and not as a stand-alone technical report.

The following component part numbers comprise the compilation report:
ADP012853 thru ADP013001

Electronic properties and many-body effects in quantum dots

Satyadev Nagaraja and *Jean-Pierre Leburton*

Department of Electrical & Computer Engineering and
Beckman Institute for Advanced Science & Technology
University of Illinois at Urbana-Champaign, Urbana, IL 61801, USA

Abstract. We investigate the shell structure and electron-electron interaction in planar quantum dots within the density functional theory. We observe that the Coulomb repulsion does not alter the shell structure when the dot is symmetric in the two-dimensional (2D) plane. If the dot is asymmetric, no pre-determined shell structure emerges except when Coulomb repulsion leads to accidental *Coulomb degeneracies*. Our investigations on double-quantum dots reveal double electron charging for weak inter-dot coupling, and a significant spin polarization in accordance with Hund's rule. Both these features disappear when interdot coupling is made stronger.

Introduction

Zero-dimensional (0D) systems, such as quantum dots have been the subject of intense research in recent years [1–4], owing to novel fundamental physical phenomena as well as their potential for many exciting applications in optics and electronics [5–7]. In this work, we investigate the influence of the confining potential and electron-electron interaction in the formation of shell structure in single planar quantum dots (PQD), and the role of many body interaction, especially the effect of electron spin, on the charging behavior of coupled PQDs. Planar quantum dots are defined by electrostatically depleting a two-dimensional electron gas beneath negatively biased metal gates on top of the stucture. We consider two PQD configurations: a square-gate dot which, when empty, has a nearly circularly symmetric confining potential, and a quad-gate dot which has a rectangular symmetry. Additionally, we investigate the charging properties of a double PQD.

1 Dot structures

The devices investigated here are shown in Fig. 1 (notice the $y-$axis is in the vertical direction). They consist of an inverted GaAs/Al$_{0.3}$Ga$_{0.7}$As heterostructure which confines the electrons to a 2D gas at the interface. In our model, the simulated structure consists of a 22.5-nm layer of undoped Al$_{0.3}$Ga$_{0.7}$As, followed by a 125-nm layer of undoped GaAs and finally an 18 nm GaAs cap layer. The cap layer is uniformly doped to 5×10^{18} cm^{-3} so that the conduction band edge is just above the Fermi level at the GaAs-cap layer–undoped GaAs boundary. The inverted heterostructure is grown on a GaAs substrate and charge control is achieved by varying the voltage on the back gate, V_{back}. The first quantum dot shown in Fig. 1(a) has a 240×240 nm^2 square open area at the top bordered by a 65-nm thick gate. The quad-gate device shown in Fig. 1(b) has four gate pads with 45-nm stubs protruding into the channel; the dimensions of the open area on the top are 230×408 nm^2. The separation between the pads along the (longer) $z-$direction is 90-nm. The schematic of the coupled dot structure is shown in Fig. 1(c). The two dots are defined by biasing the ten metallic gates, with the coupling between them varied by means of the voltage, V_t, on the tuning gates.
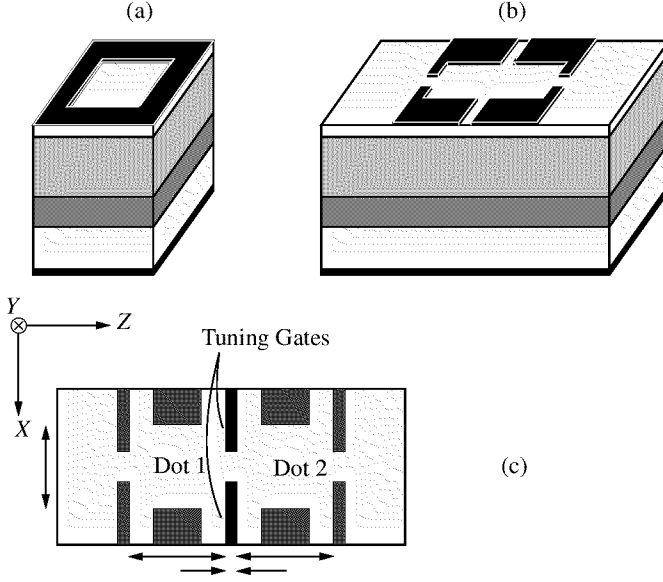
Fig. 1. Schematic representation of (a) a square and (b) a quad gate quantum dot device with layer structure (c). Schematic representation along the $x - z$ plane.

2 Computational model

In order to study the electronic properties of the quantum dot, the 3D Schrödinger and Poisson equations are solved for the central 0D region within the density functional theory [ ]. The Hamiltonian ($\hat{H}^{\uparrow}$ and $\hat{H}^{\downarrow}$ for spin $\uparrow$ and spin $\downarrow$ electrons, respectively) is given by:

$$\hat{H}^{\uparrow(\downarrow)} = -\frac{\hbar^2}{2}\nabla\left[\frac{1}{m^*(\mathbf{r})}\nabla\right] + E_c(\mathbf{r}) + \mu_{xc}^{\uparrow(\downarrow)}[n, \zeta] \tag{1}$$

where $m^*(\mathbf{r})$ is the position dependent effective mass of the electron in the different materials, $E_c(\mathbf{r}) = \phi(\mathbf{r}) + \Delta E_{os}$ the conduction band edge, where $\phi(\mathbf{r})$ is the electrostatic potential, and ΔE_{os} the conduction band offset. $\mu_{xc}^{\uparrow(\downarrow)}[n, \zeta]$, the exchange and correlation potential, is a functional of the total electron density $n(\mathbf{r})$ ($= n^{\uparrow}(\mathbf{r}) + n^{\downarrow}(\mathbf{r})$) and the spin polarization parameter $\zeta = \frac{n^{\uparrow}(\mathbf{r}) - n^{\downarrow}(\mathbf{r})}{n^{\uparrow}(\mathbf{r}) + n^{\downarrow}(\mathbf{r})}$, and has been parametrized by Ceperley and Alder [ ].

The 3D Poisson equation for the electrostatic potential $\phi(\mathbf{r})$ reads:

$$\nabla[\epsilon(\mathbf{r})\nabla\phi(\mathbf{r})] = -\rho(\mathbf{r}) \tag{2}$$

where, the charge density $\rho(\mathbf{r})$ is given by $e[p(\mathbf{r}) - n(\mathbf{r}) + N_D^+(\mathbf{r}) - N_A^-(\mathbf{r})]$. Here, $\epsilon(\mathbf{r})$ is the permittivity of the material and a function of $y-$ only throughout this work, $p(\mathbf{r})$ the hole concentration, $n(\mathbf{r})$ the total electron concentration, and $N_D^+(\mathbf{r})$ and $N_A^-(\mathbf{r})$ the ionized donor and acceptor concentrations, respectively.

The Schrödinger equation is solved self-consistently with the Poisson equation by the Iterative Extraction Orthogonalization Method (IEOM) [ ]. A detailed discussion of these methods and as well as the schemes employed to determine the number of electrons at equilibrium may be found in references [ ] and [ ].
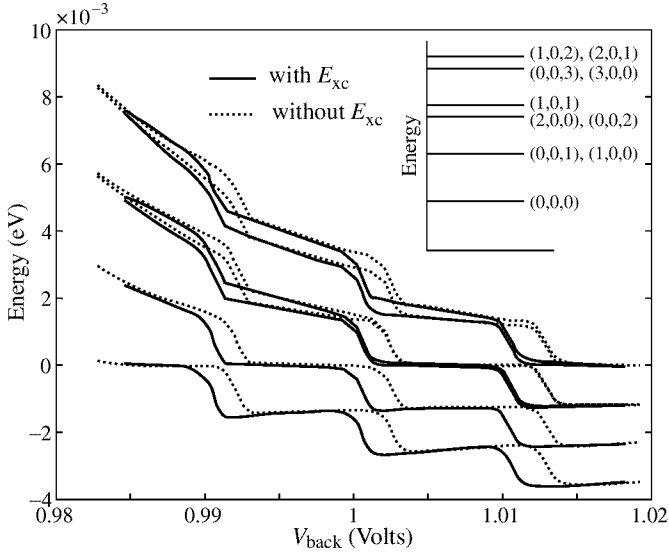
Fig. 2. Variation of the single-particle energy levels with V_{back} for the square-gate dot. The zero of the energy scale corresponds to the Fermi level. The inset shows the schematic of the energy spectrum for the empty ($N = 0$) dot with level ordering.
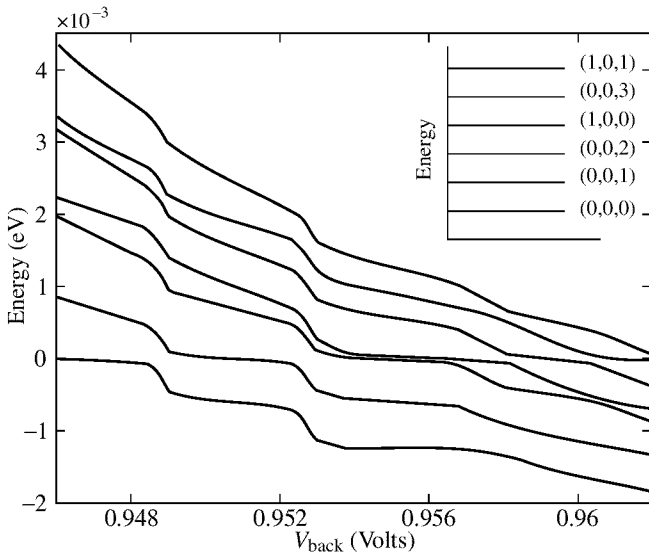
Fig. 3. Variation of the single-particle energy levels with V_{back} for the square-gate dot. The zero of the energy scale is the Fermi level. The inset shows the schematic of the energy spectrum for the empty ($N = 0$) dot with level ordering.

3   Results

### 3.1   Single quantum dots: shell structure vs. electron-electron interaction

It is well known that the conduction band edge for a grid-gate dot is quasi-parabolic at low energies for $N = 0$ [13, 14].

The evolution of the single-particle energy levels as a function of V_{back} is illustrated in Fig. 2 which shows a staircase variation of the first ten levels. Individual spin states have not been resolved in this diagram. It is seen that at $V_{back} = 0.985$ V the levels are well separated, but when the ground state, $(0, 0, 0)$ [15], crosses the Fermi level, it "sticks" to this levels over a voltage range which corresponds to the charging of the first two electrons in the dot. This produces a change in slope of the upper levels which remain well separated from the first level. Meanwhile, the third and fourth levels which are respectively threefold and fourfold degenerate, and accomodate up to 6- and 8-electrons, each split into two new levels. This effect is due to the Coulomb interaction between carriers which induces some anharmonicity in the confining potential and lifts the degeneracy of the (101)-state with the (200)- and (002)-states, on one hand, and the degeneracy of the (201)- and (102)-states with the (003)- and (300)-states on the other (Fig. 2 inset). However, because of the conservation of the square symmetry of the (002)- and (200)-, the (300)- and (003)-, and the (201)- and (102)-states remain degenerate, respectively. Also visible in Fig. 2 is the influence of electron exchange-correlation which shifts all the single particle levels to lower energy because of the attractive nature of this many-body interaction.

In contrast to the square-gate dot, the quad-gate dot depicted in Fig. 1(b), has no energy level degeneracies due to its rectangular geometry, and hence no shell structure as shown schematically in the inset of Fig. 3 with the ordering of the energy levels. Fig. 3 shows the variation of the single-particle energy spectrum with V_{back} for the quad-gate dot. The variation is qualitatively similar to the square-gate device except that each curve now represents a spin-degenerate level which reduces the shell structure to a simple superposition of doubly degenerate (due to spin) states. Because the ratio between the sides of the rectangle is incommensurable, accidental degeneracies of states are absent from this spectrum for $N = 0$. However, they do appear for higher N as the electron-electron interaction distorts the self-consistent potential. One such instance is seen for 0.943 V $\leq V_{back} \leq 0.946$ V, where the third and fourth energy levels which converge at low bias cannot cross over on the Fermi level during the charging of the dot. The anamolous "Coulomb degeneracy" is caused solely by the repulsive Coulomb interaction between levels.

3.2   Double dot

Figure 4(a) shows the *Coulomb staircase* indicating the variation of the number of electrons in the double dot (Fig. 1(c)) with V_{back} at $V_t = -0.67$ V. For $V_{back} = 0.9769$ V, $\epsilon_{LAO}(0.5)$ is just negative, implying that the dot can accept one electron in the lowermost $1s-$like state. Since the interdot coupling is very weak each of the dots can be charged simultaneously with an electron each of spin $\uparrow$ resulting in N jumping from zero to two. This simultaneous (double) charging persists as long as the two dots are isolated. However, as V_{back} is increased to 0.9804 V, when the next charge degeneracy point occurs, only one of the dots can be charged (with a $\downarrow$ electron) but not both, due to increased Coulomb repulsion between the dots. Overcoming this repulsion requires a 0.1 mV increment in V_{back} resulting in the termination of double charging, which is evident as a narrow step for $N = 3$. At $V_{back} = 0.9805$ V, Dot 2 also can be charged with a $\downarrow$ electron increasing N to 4. Similar behavior is seen for 5th and 6th spin $\uparrow$ electrons, which occupy the first excited (p_z-like) states in Dots 1 and 2, respectively. The Coulomb repulsion between them is overcome
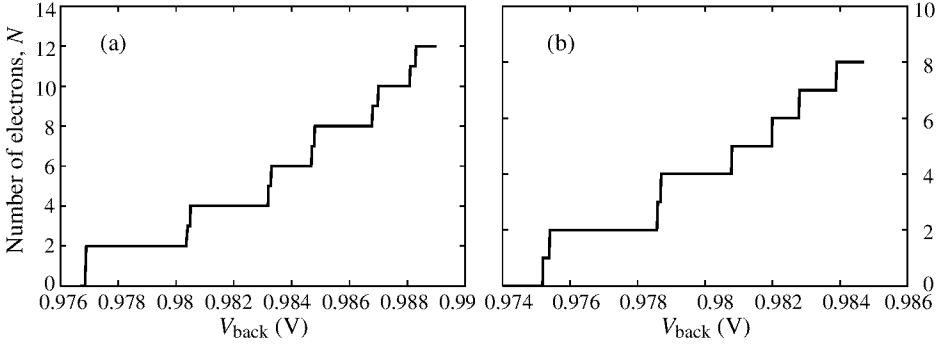
Fig. 4. Coulomb staircase diagram for the double-dot for (a) $V_t = -0.67$ V. The transitions that do not follow Hund's rules are shown in dashed lines. (b) $V_t = -0.60$ V.
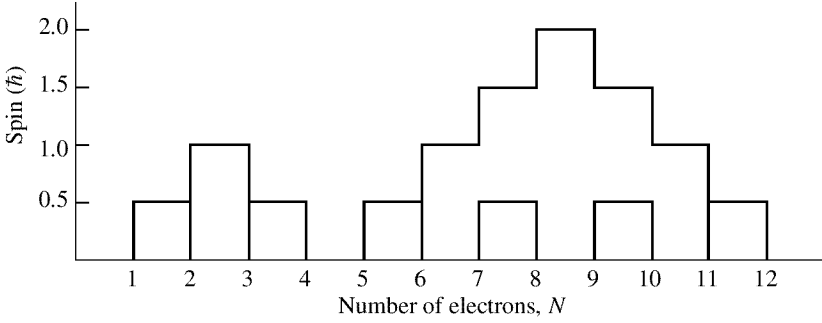
Fig. 5. Variation of the total electron spin S in the double dot with N for $V_t = -0.67$ V (solid line) $V_t = -0.60$ V (dashed line).

by a 0.1 mV increment in V_{back}. Using Hund's rule arguments, the 7th and 8th electrons are also of ↑ spin occupying the degenerate p_x−like states in Dots 1 and 2 [ ]. Thus the ground state configuration for $N = 8$ is spin polarized with four electrons having ↑ spin. The $N = 9$ through $N = 12$, complete the half occupied second shells in the two dots eventually reverting the double dot system to an unpolarized state. When the interdot coupling is increased, as in Fig. 4(b), by making V_t more positive, double charging disappears. So also spin polarization in the dot, as the energy levels are reordered and the degeneracies of the first excited states in both the dots are lifted. Fig. 5 shows the variation of total spin in the dot for $V_t = -0.67$ V and $V_t = -0.60$ V. For weak coupling the total spin of the dot increases in steps of $\hbar/2$ from 0 at $N = 5$ to $2\hbar$ at $N = 8$ as the second shell in each of the dots is half filled with spins of all the electrons being parallel. For an increase in the coupling strength between the dots such a spin polarization of the dot is precluded by a lifting of degeneracy of the p_x- and p_z-states of the first shell and the total spin is never greater than $\hbar/2$.

4 Conclusions

We have investigated the shell structure in planar single quantum dots and observed that it remains largely unaltered by electron-electron interaction when the dots have a cylindrical

symmtery, but are drastically altered and lead to accidental degeneracies when the two-dimensional symmetry is lacking. In double-PQDs, we observe double electron charging for weak inter-dot coupling, which is terminated as the coupling increases. Furthermore, in the weak coupling regime, the dot becomes strongly spin polarized for $N = 8$ in accordance with Hund's rules. An increase in inter-dot coupling reverts the dot into an unpolarized spin state.

Acknowledgements

References

 [1] C. W. J. Beenakker, *Phys. Rev. B* **44**, 1646 (1991).
 [2] D. V. Averin, A. N. Korotkov and K. K. Likharev, *Phys. Rev. B* **44**, 6199 (1991).
 [3] U. Meirav and E. B. Foxman, *Semicond. Sci. Tech.*, **10**, 255 (1995).
 [4] R. J. Haugh, R. H. Blick and T. Schmidt, *Physca B* **212**, 207 (1995).
 [5] D. Leonard, K. Pond and P. M. Petroff, *Phys. Rev. B* **40**, 11687 (1994).
 [6] K. Imamura, Y. Sugiyama, Y. Nakata, S. Muto and N. Yokoyama, *Jpn. J. Appl. Phys* **34**, 1445 (1995).
 [7] J. Jimenez, L. R. C. Fonseca, D. J. Brady, J. P. Leburton, D. E. Wohlert and K. Y. Cheng, *Appl. Phys. Lett.* **71**(25), 3558 (1997).
 [8] R. O. Jones and O. Gunnarsson, *Rev. Mod. Phys.* **61** (3), 689–746 (1989).
 [9] J. P. Perdew and Z. Zunger, *Phys. Rev. B* **23**, 5048 (1981).
[10] R. Kosloff and H. Tal-Ezer, *Chem. Phys. Lett.* **127**, 223 (1986).
[11] D. Jovanovic and J. P. Leburton, *Phys. Rev. B* **49**, 7474 (1994).
[12] S. Nagaraja, J. P. Leburton and R. M. Martin, *unpublished* 1999.
[13] A. Kumar, S.E. Laux and F. Stern, *Phys. Rev. B* **42**, 5166 (1990).
[14] S. Nagaraja, P. Matagne, J. P. Leburton, Y. H. Kim and R. M. Martin, *Phys. Rev. B* **56**, 15572 (1997).
[15] we follow the (n_x, n_y, n_z) representation of the wavefunction with n_x, n_y and n_z representing the number of nodes of the wavefunctions along $x-$, $y-$, and $z-$ directions, respectively.
[16] S. Tarucha, D. G. Austing, T. Honda, R. J. van der Hage and L. P. Kouwenhoven, *Phys. Rev. Lett.* **77**, 3613 (1996).